Surface characterisation of dextran-coated iron oxide nanoparticles prepared by laser pyrolysis and coprecipitation

M. Carmen Bautista, Oscar Bomati-Miguel, María del Puerto Morales, Carlos J. Serna, Sabino Veintemillas-Verdaguer*

Instituto de Ciencia de Materiales de Madrid, CSIC, C) Sor Juana Inés de la Cruz 3, Cantoblanco, 28049 Madrid, Spain

Available online 5 March 2005

Abstract

The favoured mechanism of adsorption of dextran on the surface of maghemite nanoparticles (5 nm) prepared by laser pyrolysis seems to be the collective hydrogen bonding between dextran hydroxyl groups and iron oxide particle surface. After heating, the formation of a surface complex between the polysaccharide oxygen atoms and the surface iron atoms gave rise to a stronger bonding.
© 2005 Elsevier B.V. All rights reserved.

Keywords: Laser pyrolysis; Iron oxide; Nanoparticles; Dextran coating; Thermal analysis; Infrared spectroscopy; Maghemite

1. Introduction

Biocompatible colloids based on nanometric superparamagnetic iron oxide nanoparticles have a wide range of biomedical and diagnostic applications [1–3]. To ensure stability and reproducible performance of the colloids, it is important to monitor and control their composition and uniformity. Stability, biocompatibility and relaxometric properties of these iron oxide colloids are affected by their particle size distribution as well as by the surface coating of the particles in the solution [4]. These parameters depend on the nanoparticles synthesis procedure and the colloid preparation method. The most commonly used synthesis of superparamagnetic iron oxide is the coprecipitation of iron salts in the presence of a base [5]. Recently a new method to produce magnetic nanoparticles has been developed in our laboratory by laser-induced pyrolysis of pentacarbonyl iron vapours [6]. Unlike the coprecipitation method, laser pyrolysis allows one to obtain bare iron oxide particles with monomodal size distributions in the range between 5 and 10 nm in a single step.

The stability of the colloid suspensions is greatly improved by the addition of suitable polymeric

*Corresponding author. Tel.: +34 91 3349061; fax: +34 91 3720623.

E-mail address: sabino@icmm.csic.es (S. Veintemillas-Verdaguer).

dispersants [7]. In the case of magnetic nanoparticles, these polymeric additives can induce an interparticle repulsion that counteracts the magnetic attraction between particles. The adsorbed polymer layer should be thick enough to prevent the particles from coming in close contact and be firmly "anchored" to the surface of the particles to avoid degradation of the fluid with time. Moreover, for biomedical applications, the adsorbed polymer layer should completely cover the particles and be as dense as possible in order to protect the iron oxide core against contact with blood proteins and phagocytosis-associated receptors [8]. The most common coatings for biocompatible iron oxide based colloids are derivatives of dextran or polyethylene glycol [9,10]. Dextran is a polymer $(C_6H_{10}O_5)_n$, of anhydroglucose having mainly alpha-D(1-6) linkages with some unusual 1,3 glucosidic linkages at branching points. In aqueous solutions, dextran interacts with metals and covers its surface yielding aggregates with hydrodynamic diameters between 20 and 150 nm [11]. Magnetic nanoparticles prepared by laser pyrolysis have been also successfully coated with dextran and it was shown to form aggregates of around 50 nm with similar blood residence times to commercial products of similar composition prepared by coprecipitation in the presence of dextran (called SPIO) [12,13]. However, so far not many works about the nature of the interaction of the dextran with the iron oxide surface have been published [14], in spite of being an important issue affecting the residence time of the nanoparticles in the blood before its clearance and, therefore, its actuation time.

The work reported here, described dextran surface modification of pure superparamagnetic iron oxide nanoparticles prepared by laser pyrolysis and by coprecipitation method. Physical characterisation techniques, including electrophoretic mobility, thermal analysis, and mass and infrared spectroscopy, were used in this study to delineate the nature and the mechanism of dextran particulate adsorption.

2. Method and experiment

Pure iron oxide particles were obtained by laser-induced pyrolysis of iron pentacarbonyl vapours in ethylene (sample P) following the method previously reported [6]. For comparison, magnetic nanoparticles obtained by coprecipitation of Fe(II) and Fe(III) salts in the presence of K(OH) at 0 °C were used in this study and named as sample C [5,15]. Magnetic characterisation of these samples, P and C, was carried out at room temperature by using a vibrating sample magnetometer (MLVSM9 MagLab 9 T, Oxford Instrument) and a maximum applied field of 5 T.

Aqueous colloidal dispersions of both samples were obtained by slow addition of a suspension composed by 200 mg of iron oxide nanoparticles in 2.5 ml of 0.5 M NaOH to a solution composed by 200 mg of dextran in 2.5 ml of 0.5 M NaOH. The addition was made under sonication for 30 min and the resultant suspension remained under sonication for 24 h at 30 °C. Afterwards the dark brown dispersion obtained is immediately dialysed in 5 l of distilled water for 24 h by using a 12,000–14,000 nominal molecular weight cut off membrane and finally filtrated under 0.22 μm size. The dextran $(C_6H_{10}O_5)_n$ had a molecular weight of ~6000 purchased from Fluka Biochemika and it was used without further purification.

The dispersion of dextran-coated nanoparticles prepared using the laser pyrolysis sample (P) by the method described above is named sample DP, and the homologous dispersion obtained from coprecipitation sample (C) using the same method is named sample DC.

The final concentration of the dispersions was determined by total reflection X-ray fluorescence (TXRF) using a Seifert EXTRA-II spectrometer.

Transmission electron micrographs were obtained using a JEOL JEM-2000FX microscope (TEM) operated at 200 keV. Samples were prepared by spray-drying drops of diluted solutions of the suspensions on carbon films supported by copper grids. Aggregate size distribution was obtained by measuring the calliper diameter of at least 100 aggregates.

Hydrodynamic diameter of the aggregates, considering the magnetic cores and the coating, was calculated by photon correlation spectroscopy (PCS), in a ZETASIZER 1000 HS from Malvern Instruments.

The electrophoretic mobility of the colloidal dispersion as a function of the pH was measured in 10^{-2} M KNO$_3$ background electrolyte solution using a COULTER DELSA 440. The set of predetermined pH values was adjusted using KOH and HNO$_3$ solutions.

The samples employed for thermogravimetric and infrared studies were obtained by drying the dispersions at 50 °C during 24 h. Thermogravimetric analysis was performed in a Seiko, TG/DTA EXSTAR 6000 thermobalance by heating the samples from 25 to 1000 °C at 5 °C min^{-1} under a nitrogen flow of 150 ml min^{-1} in order to avoid violent dextran oxidation. The exit gases were analysed with a thermostar quadrupole mass spectrometer (PFEIFFER) coupled with the former thermal analysis apparatus. Fourier transform infrared spectroscopy (FTIR) spectra were measured using a BRUKER IFS 66v/S spectrometer. The original and heated at 200, 300, 500 °C samples were mixed with KBr and pressed. Their spectra were recorded over the frequency range from 250 to 4000 cm^{-1} and their changes in the spectra were compared with the thermal analysis results.

3. Results and discussion

Iron oxide (probably maghemite γ-Fe$_2$O$_3$) nanoparticles of 3.7 ± 2 nm in diameter, as determined by TEM, were obtained by laser pyrolysis [6]. The magnetic behaviour of this sample is superparamagnetic at room temperature with a saturation magnetisation value of 28 emu g^{-1} [13]. The method used to coat the magnetic nanoparticles with dextran led to a highly homogenous suspension consisting of aggregates of particles as it can be observed in Fig. 1 (sample DP). The final concentration of the dispersion was 11 mg Fe ml^{-1} (11,000 ppm). From electron micrographs at higher magnification, a mean aggregate size of 28 ± 22 nm was obtained (data not shown). Comparing this value with the hydrodynamic size obtained from photon correlation spectroscopy (46 ± 29 nm), a dextran layer thickness of around 10 nm can be estimated. This means that these suspensions fit the requirements for being injected
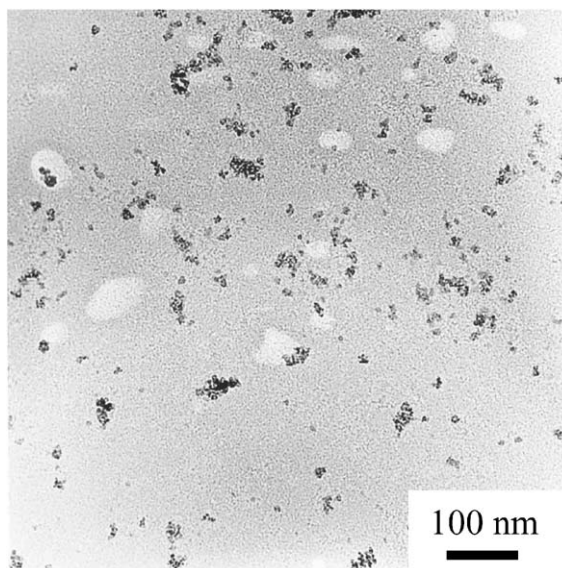

Fig. 1. Low-resolution TEM photographs of the dextran-coated iron oxide nanoparticles obtained by laser pyrolysis (DP).

intravenously (hydrodynamic diameter less than 150 nm). Dextran coating thickness between 8 and 12 nm, have been observed for stable colloidal suspensions of magnetic nanoparticles [12]. For comparison, sample C of bare oxide particles of 8 ± 2 nm in diameter was prepared by coprecipitation and it also showed superparamagnetic behaviour at room temperature and a saturation magnetisation of 50.5 emu g^{-1} [15]. Special difficulties appeared in the dispersion and coating of this sample according to its larger saturation magnetisation to give rise to stable colloidal suspension of the magnetic nanoparticles (sample DC). The attained final iron concentration in sample DC was only 60 ppm Fe, with a mean aggregate sizes observed by TEM of 57 ± 17 nm, and a hydrodynamic size of 214 ± 80 nm.

Moreover, the adsorption of dextran on the laser pyrolysis powder seems to be a continuous process as it is shown in Fig. 2. The hydrodynamic size of the dispersions, incubated after the sonication step is observed to increase linearly with time until precipitation arises. This means that under the strong alkaline media employed not only a particle–dextran interaction takes place but also
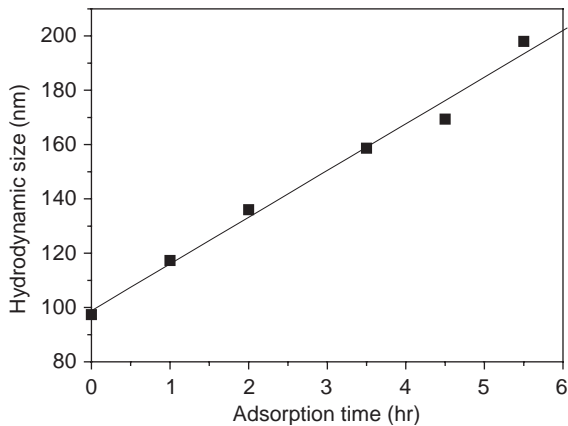
Fig. 2. Variation of the hydrodynamic size of the dextran-coated nanoparticles prepared by laser pyrolysis as a function of adsorption time.
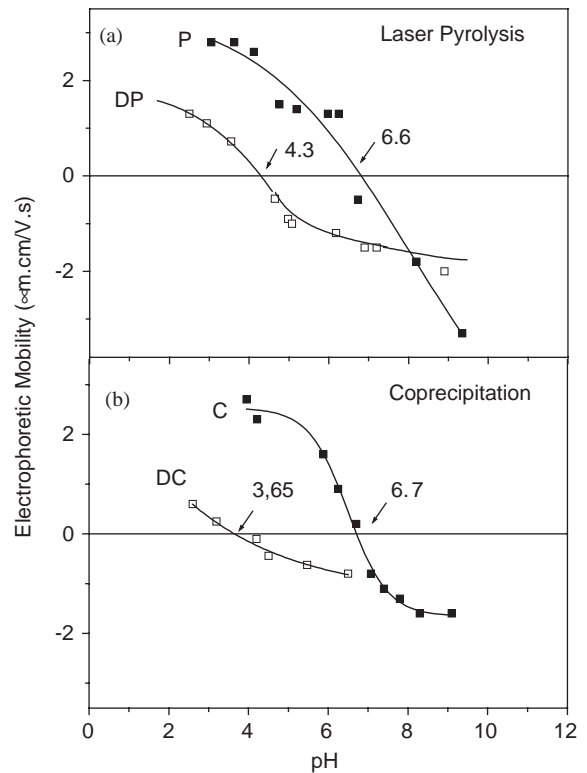

Fig. 3. Electrophoretic mobility versus pH measured for uncoated and dextran-coated iron oxide nanoparticles prepared by laser pyrolysis (a) and by coprecipitation (b).

dextran–dextran interactions beyond the first adsorption layer.

After the adsorption process, alcoholic hydroxyl groups belonging to the adsorbed dextran are present on the surface of the coated particles, instead of the hydroxide groups presented on the bare iron oxide surface. This difference is reflected in the pH dependence of the electrophoretic mobility (Fig. 3). From this dependence the isoelectric point (the pH of zero mobility) is obtained. At this pH the surface concentration of negative O^- and positive OH_2^+ surface groups is equal. For the uncoated (samples P and C), the isoelectric point is 6.6 and 6.7 as reported [16], but an important decrease of this parameter to 4.3 and 3.6 for coated samples DP and DC, respectively. This reflects the lower acidity of organic alcohol groups with respect to their inorganic hydroxyl counterpart. An important consequence of this fact is that the dextran coated particles have negative surface charge in the pH range between 4 and 10 and therefore they will be stable at the physiological pH ≈ 7 one of their minimum prerequisites for their use in biomedical applications.

In order to analyse the nature of the bonding between the dextran and the particle surface of iron oxide and its evolution with temperature, thermogravimetric and differential thermal analyses for the bare iron oxide nanoparticles (P, C)

and the gentle dried suspensions of coated nanoparticles (DP, DC) were carried out. These techniques are powerful and widely used tools for studying and characterising polymers [17]. Distinctive weight losses for samples P and DP are evident from Fig. 4a. Three temperature ranges can be established: 25–200, 200–500 and 500–1000 °C. Thus, magnetic nanoparticles (samples P, C) show a very small weight loss of around 14%, which takes place mainly up to 500 °C and is attributed mainly to hydrogen groups as a consequence of the high surface of the nanoparticles.

However, the thermogravimetric curve for dextran-coated particles (samples DP) shows significant differences. First, a total weight loss of 64% takes place during the thermal heating from room temperature to 1000 °C. The 9% weight due to physically adsorbed water is lost in the first
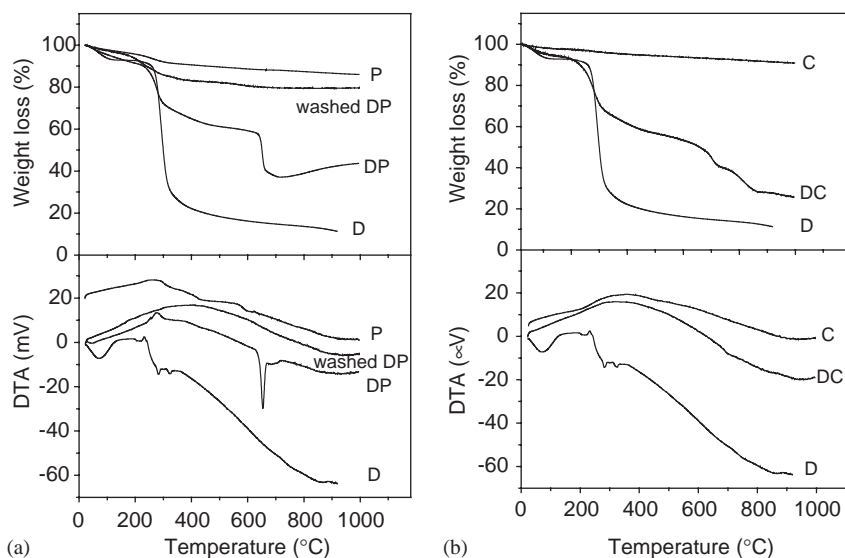
Fig. 4. (a) TG-DTA curves of samples prepared by laser pyrolysis: iron oxide nanoparticles (P), dextran-coated iron oxide nanoparticles (DP), dextran (D) and washed-DP. (b) TG-DTA curves of samples prepared by coprecipitation: iron oxide nanoparticles (C), dextran-coated iron oxide nanoparticles (DC) and dextran (D).

temperature range, and around 30% and 25% in the 200–500 and 500–1000 °C intervals, respectively. The last two steps are associated to an exothermic peak at 260 °C and an endothermic one at 665 °C as observed in the DTA (Fig. 4a). Exothermic reactions are expected when oxidation takes place, while endothermic reactions appear when decomposition occurs. Although this experiment has been carried out in a nitrogen atmosphere, the presence of some oxygen cannot be discarded. Thus, it seems that the first exothermic peak is the result of simultaneous oxidation and decomposition of unmodified dextran molecules due to its temperature coincidence with the temperature reported in the literature for free polysaccharides (230–400 °C [18]) for the same process, see also TG-DTA curves for dextran (sample D) in Fig. 4a,b. However, the second endothermic peak at higher temperature for sample DP seems to be the result of a predominant decomposition process of dextran molecules strongly liked to the particles.

The removal of organic material at this high temperature has been confirmed by the analysis of the gases emitted by mass spectroscopy coupled to the thermal analysis. During the heating of sample DP the detection of CO_2 and H_2O are coincident with the position of the TG-DTA peaks in both the low and high temperature range (Fig. 5).

In order to clarify whether the strong bonding is originated in the low temperature coating process or is generated during the heating process, the sample DP was diluted with 10 times its volume of distilled water and concentrated again by centrifugation three times. The resulting sample showed a thermal behaviour similar to the bare sample P (Fig. 4a), reflecting the almost total elimination of the dextran coating in the washing process. Therefore, the stable covalent bond between the dextran molecules and the particle surface detected by TG-DTA in these samples seems to be originated during the heating process. A sample gentle dried and heated at 300 °C (5 °C/min) did not show dextran loss after washing under the same conditions (data not shown).

Thermogravimetric and TG-DTA analysis of samples C and DC, Fig. 4b, showed similar weigh losses that those showed for the previously described pyrolysis samples P and DP. The main difference was found in the TG and DTA curve for sample DC in the high temperature range 500–1000 °C. In this case, the dextran-coated
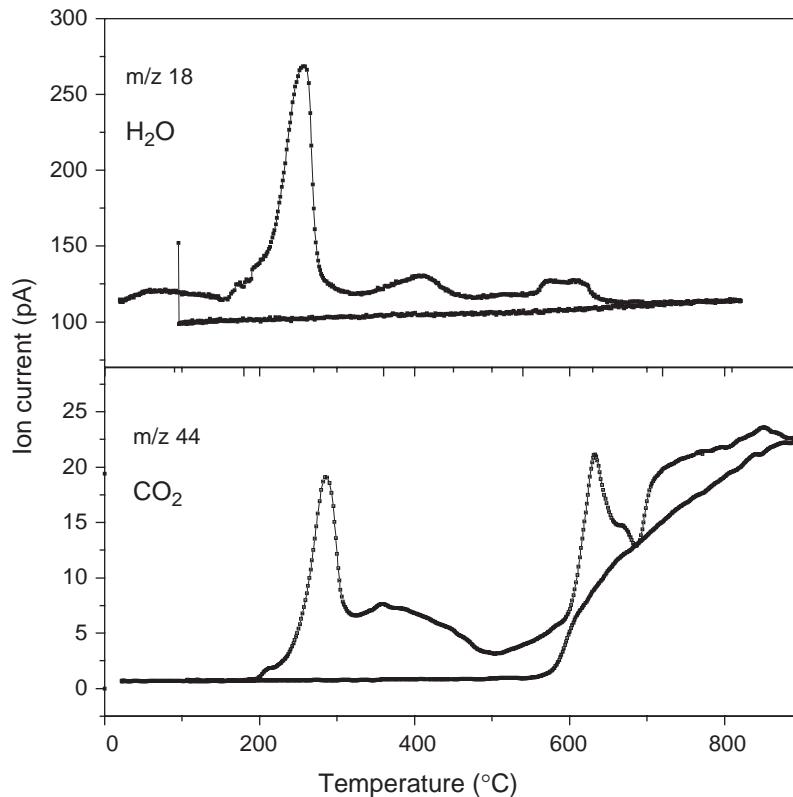
Fig. 5. Qualitative analysis by mass spectrometry of the gases evolved during the heating of dextran-coated laser produced iron oxide nanoparticles, sample (DP).

particles losses around 30% in two steps, at 700 and 812 °C. However, no endothermic peak associated with this weight loss was found in the DTA (Fig. 4b). This means that the strong bond generated between the dextran and the nanoparticles upon heating is absent or much diminished in the DC sample reflecting the dependence of the nanoparticle surface reactivity on the preparation method.

The dextran coating was also studied by the FTIR spectroscopy. Fig. 6 shows the spectra for uncoated (P) and coated (DP) iron oxide nanoparticles. The spectrum for dextran (D) is also included in the same figure for comparison. This spectrum exhibits the polysaccharide characteristic absorption bands such as $3412 \, cm^{-1}$ due to the O–H stretching, $1647 \, cm^{-1}$ due to water molecule bending, 2926, 1420 and $1358 \, cm^{-1}$ assigned to v(C–H) and δ(C–H) vibrational modes, 1156 and

1010 due to C–O vibrations and the bands at 916, 852 and $764 \, cm^{-1}$ corresponding to α-glucopyranose ring deformation modes [14]. Iron oxide nanoparticles (P) also show O–H strong absorption bands at around $3500 \, cm^{-1}$ because of the water physically adsorbed. In addition, two broad bands placed at about 583 and $441 \, cm^{-1}$ correspond to Fe–O vibration modes in partially disordered γ-Fe_2O_3 particles, which is the case of particles prepared by pyrolysis of a vapour or aerosol [6,19].

For the dextran-coated particles (DP), infrared spectra were recorded after heating at 50, 200, 300 and 500 °C for half an hour (Fig. 6). These temperatures were selected on the basis of the TG-DTA results. Significant band shifts between non-adsorbed and adsorbed polysaccharides on hematite have been observed in the region below $1000 \, cm^{-1}$ [20]. Unfortunately in this work,

dextran bands in that region are overlapped by the Fe–O bands. The rest of the dextran bands showed no spectral changes upon coating (sample DP-50). Based on this result and the reversible nature of the dextran adsorption reflected by their easy removal from the surface by washing with water, collective hydrogen bonding between dextran hydroxyl groups and iron oxide particle surface seems to be the most probable mechanism of adsorption at low temperature (Fig. 7). Similar adsorption mechanism was proposed for dextran-coated maghemite nanoparticles obtained by coprecipitation where no change in the IR spectrum was also observed [14]. As sample DP
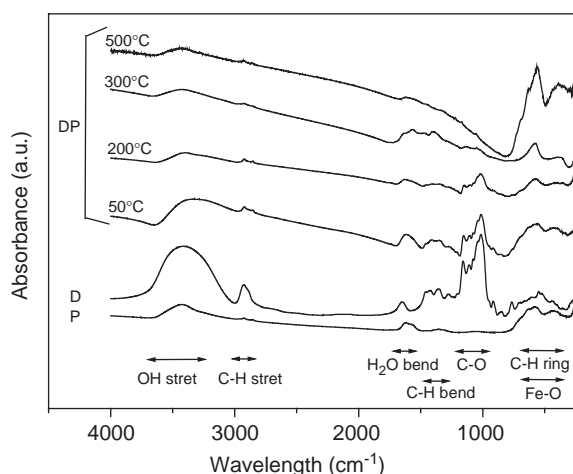

Fig. 6. FTIR spectra of dextran (D), iron oxide nanoparticles prepared by laser pyrolysis (P), and dextran-coated iron oxide nanoparticles (DP) heated at 50, 200, 300 and 500 °C.

is heated at higher temperatures, two main features can be observed in the IR spectra. First, the OH stretching band at $3318\,cm^{-1}$ is clearly diminished, which suggests a reduction in the number of hydroxyl groups and therefore a reduction in the number of hydrogen bonds. Second, in the region between 1500 and $1000\,cm^{-1}$, the sharp bands observed in the free dextran spectrum are found to be merged and broadened upon heating above 300 °C. Although, the precise assignment of these dextran bands is not possible as all the vibrations in this region are highly coupled, the spectral modification suggests the formation of a surface complex between the polysaccharide oxygen atoms and the surface iron atoms. Previous studies of the reactivity of different polar groups with maghemite has shown that the functional group anchored to the surface through chemical bond formation is the carboxylic group, transforming the carboxylic acid functionality to a carboxylate functionality with both oxygen atoms interacting with the metal on the surface [21] (Fig. 7). In our case the partial oxidation of the adsorbed dextrane at temperatures between 200 and 500 °C can generate these carboxylic groups from the original aldehyde groups present in the linear form of the glucose.

The reason for the different reactivity of the iron oxide samples produced by laser pyrolysis in the gas phase (P) and obtained by coprecipitation in solution (C) could be related to the higher hydration of sample C. The additional water present in this case could remain at high temperatures and protect the
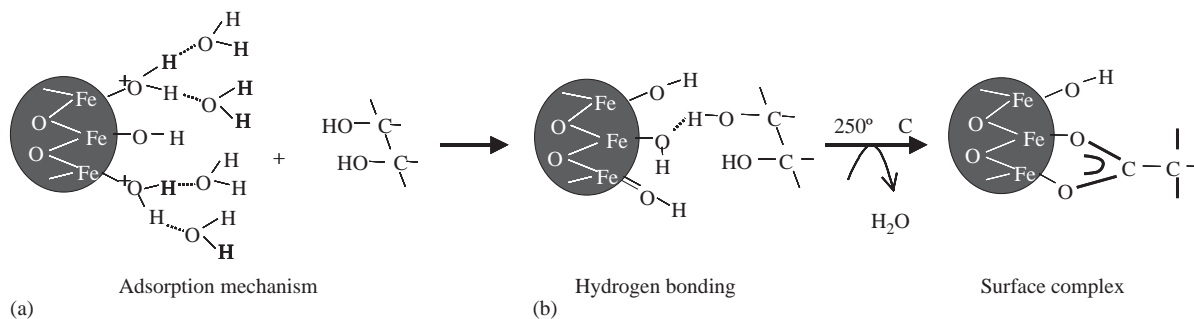

Fig. 7. Schema of the hypothetical process that takes place during heating dextran coated iron oxide nanoparticle prepared by laser pyrolysis. (a) At low temperatures, water lies between the oxide surface and the dextran forming a network of hydrogen bridges. (b) After heating, water is partially eliminated, oxidation takes place and direct carboxylate bonds between dextran and iron oxide have the chance to be formed.

particle surface from the dextran preventing the formation of a direct bond (Fig. 7).

The heating process mentioned could be an alternative to the dextran crosslinking actually employed to stabilize the dextran coating that uses epichlorydrine (a toxic reagent) [22].

4. Conclusions

Iron oxide dispersions produced by alkaline dextran adsorption on maghemite nanoparticles under sonication stirring were studied by means of their electrophoretic mobility in liquid state, and thermogravimetry and infrared spectroscopy after drying. Differences in the results were obtained depending on the synthetic procedure for the preparation of the nanoparticles. In particular, better dispersions were attained by laser pyrolysis synthesized oxide (P) in comparison with coprecipitation oxide (C). Additionally, the formation of a strong bond between dextran and the iron oxide during heating of the dry samples of the suspensions prepared using laser produced powders (DP) was detected. This bond is not formed in the case of the suspensions prepared using precipitation powders (DC). The obtained results suggest the convenience of developing dextran coating procedures of the iron nanoparticles at higher temperatures and perhaps short times (to avoid dextran decomposition) in order to obtain permanent linkage of dextran to the particles.

Acknowledgements

References

[1] Q.A. Pankhurst, J. Connolly, et al., J. Phys. D 36 (2003) R167.
[2] P. Tartaj, M.P. Morales, et al., J. Phys. D 36 (2003) R182.
[3] C.C. Berry, A.S.G. Curtis, J. Phys. D 36 (2003) R198.
[4] U. Häfeli, W. Schütt, J. Teller, M. Zborowski, Scientific and Clinical Applications of Magnetic Carriers, Plenum Press, New York, 1997.
[5] L. Babes, B. Denizot, G. Tanguy, et al., J. Colloid Interface Sci. 212 (1999) 474.
[6] S. Veintemillas-Verdaguer, M.P. Morales, C.J. Serna, Mater. Lett. 35 (1998) 227.
[7] P.C. Hiemenz, R. Rajagopalan, Principles of Colloid and Surface Chemistry, Marcel Dekker Inc., New York, 1997.
[8] R. Weissleder, A. Bogdanov, et al., Adv. Drug Delivery Rev. 16 (1995) 321.
[9] R.S. Molday, D. Mackenzie, J. Immunol. Methods 52 (1982) 353.
[10] Y. Zhang, N. Kohler, M. Zhang, Biomaterials 23 (2002) 1553.
[11] T.T. Shen, R. Weissleder, et al., Magn. Reson. Med. 29 (1993) 599.
[12] M.C. Bautista, O. Bomati-Miguel, et al., Nanotechnology 15 (2004) S154.
[13] S. Veintemillas-Verdaguer, M.P. Morales, et al., J. Phys. D 37 (2004) 2054.
[14] C.W. Jung, Magn. Reson. Imaging 12 (1995) 675.
[15] M.P. Morales, S. Veintemillas-Verdaguer, et al., Chem. Mater. 11 (1999) 3058.
[16] W. Stumm, J.J. Morgan, Aquatic Chemistry, second ed., Wiley, New York, 1981, p. 631.
[17] G. Bumbu, C. Vasile, et al., Polym. Degrad. Stab. 72 (2001) 99.
[18] A. Carpov, G.-G. Bumbu, et al., Cellulose Chem. Technol. 34 (2000) 451.
[19] T. González-Carreño, M.P. Morales, et al., Mater. Lett. 18 (1993) 151.
[20] P.K. Weissenborn, L.J. Warren, J.G. Dunn, Colloid Surf. A 99 (1995) 11.
[21] Q. Liu, Z. Xu, Langmuir 11 (1995) 4617.
[22] W.S. Palmacci, L. Josephson, US Patent no. 5,262,176 (1993).